Product Branching Fractions in the Reaction of NH (ND) ($^3\Sigma^-$) with NO

Joseph L. Durant, Jr.

Combustion Research Facility, Sandia National Laboratories, Livermore, California 94551

Received: August 6, 1993®

We have carried out a combined experimental and theoretical study of the reaction of NH (ND) ($^3\Sigma^-$) with NO aimed at understanding the product distribution from that reaction. The reaction was studied at room temperature using the discharge flow technique with mass spectrometric detection of the reaction products. Measured product branching fractions at room temperature for production of N_2O + H (D) were 0.8 ± 0.4 for NH ($^3\Sigma^-$) + NO and 0.87 ± 0.17 for ND($^3\Sigma^-$) + NO (1σ statistical errors). Stationary points on the HNNO $^2A'$ potential energy surface were characterized using the Gaussian 2 *ab initio* method. The initial addition of NH($^3\Sigma^-$) to NO on the $^2A'$ surface is predicted to proceed without a barrier to form *trans*-HNNO; reaction to produce the *cis* isomer is predicted to have a barrier of 2.9 kcal/mol. The *cis*- and *trans*-HNNO are predicted to be at −48.9 and −56.0 kcal/mol relative to the separated reactants. Transition states with energies of −25.3 and −17.9 kcal/mol were located for dissociation of the *cis* isomer into H + N_2O and OH + N_2, respectively. The transition state for interconversion of the isomers was calculated to be at approximately −30.8 kcal/mol. The *trans*-HNNO was found to isomerize to the *cis* form before decomposing. The potential energy surface calculated explains the major features of the reaction.

Introduction

The reaction of NH($^3\Sigma^-$) with NO is a moderately exothermic, radical–radical reaction with two thermodynamically open channels:[1,2]

$$NH(^3\Sigma^-) + NO \rightarrow H + N_2O \quad \Delta H_{rxn} = -34.7 \text{ kcal/mol} \quad (1a)$$

$$\rightarrow OH + N_2 \quad \Delta H_{rxn} = -97.6 \text{ kcal/mol} \quad (1b)$$

It has been claimed to be one of the principal sources of N_2O from combustion,[3,4a] although other flames studies have suggested that the primary product of the reaction is N_2, and little N_2O is formed. Its reaction rate coefficient has been studied before near room temperature,[5-9] in shock heated gas,[10,11] and in flame studies.[12-14] Reported room temperature rates are in the range $k(298) = (3.8–5.8) \times 10^{-11}$ cm^3/(molecules s). The reaction rate coefficient is reported to be temperature independent in the temperature range 269–377 K;[8] high-temperature reaction rate coefficients of $k(2200–3350 \text{ K}) = 2.8 \times 10^{-10} \exp(-6400/T)$ cm^3/(molecule s)[10] and $k(3500 \text{ K}) = (1.3 \pm 0.1) \times 10^{-10}$ cm^3/(molecules s)[11] have been reported. Recently, Patel-Misra and Dagdigian[15] have measured nascent OH product distributions arising from the reaction. There have been some direct studies examining the products from the reactions of NH($^3\Sigma^-$) with NO.[8-11] Harrison and co-workers looked for OH product with laser-induced fluorescence but were not successful in detecting it. Despite this negative result, they concluded that N_2 + OH was probably the major product of the reaction.[8] Yamasaki et al. report exclusive production of N_2 + OH at room temperature and claim that N_2O + H arises from the reaction of NH($^1\Delta$) with NO.[9] Mertens et al. report the branching fraction into N_2 + OH to be 0.27 ± 0.10 for $2350 \le T \le 3040$ K,[10] which is in good agreement with Yokoyama et al.'s branching fraction of 0.32 ± 0.07 at 3500 K.[11] Patel-Misra and Dagdigian's work[15] establishes OH as a direct product of the reaction but is mute as to its branching fraction.

There have been a number of theoretical studies of the HNNO $^2A'$ potential energy surface. Melius and Binkley[16] used the BAC-MP4 method to calculate reactants, products, and intermediates involved in the NH + NO reaction. Those calculations have since been revised due to newer bond additivity correction procedures; results of the newer calculations are reported in Miller and Melius[4] who also report of calculations of the product branching fraction for the reaction of NH with NO, based on the BAC-MP4 structures and geometries. Fueno et al.[17] used MRD-CI//HF/4-31G(d,p) to calculate energies for stationary points on the HNNO $^2A'$ surface, as well as the energy of the *cis* and *trans* isomers of HNNO $^2A''$, which were predicted to lie higher than the $^2A'$ states of the two isomers. Harrison and MacIagan[18] reported calculations of geometries at HF/6-31G(d), HF/6-311G(d,p), and MP2/6-31G(d) levels, with energies calculated using both MP2 and MP4 methods. More recently, Walch[19] has calculated a number of points on the HNNO $^2A'$ surface, using CASSCF/CCI. The results of these studies vary widely, although they all find that the transition state for production of H + N_2O is lower in energy than the one leading to OH + N_2.

The present study has sought to address questions concerning the products of the NH($^3\Sigma^-$) + NO reaction by a combined experimental and theoretical approach. We have carried out experiments using the discharge flow technique to directly measure products of the reaction and have used the Gaussian 2 method to characterize stationary points on the HNNO potential energy surface.

Experimental Section

Experiments were carried out in our double-injector, discharge-flow apparatus. The basic apparatus has been described in detail earlier.[20] The flow tube, a 22-mm-i.d. quartz tube, 530 mm long, was suspended vertically in a vacuum chamber constructed from 4 5/8-in. Conflat hardware. This study utilized a double injector consisting of a 6-mm-o.d. quartz tube mounted concentrically within a 13-mm quartz injector. This assembly was mounted on the flow tube axis. The flow tube ended either at the tip of a 2-mm-i.d. conical sampling nozzle for the mass spectrometer or approximately 1 cm above a 1-mm flat sampling nozzle. The flow tube was pumped out through the outer vacuum jacket, using an oil-free DryStar mechanical pump. Reagent flow rates were measured and controlled by MKS 1359 and Tylan

® Abstract published in *Advance ACS Abstracts*, December 15, 1993.

0022-3654/94/2098-0518$04.50/0

FC-2900 transducers connected to MKS 246 flow controllers. Pressures were measured with an MKS 390HA capacitance manometer and controlled with a variably-open butterfly valve connected to an MKS 252 exhaust valve controller. Total pressures of 0.75 and 2.5 Torr were used, with typical flow velocities of 1–4 m/s. Typical initial reagent concentrations were $5 \times 10^{12} \leq [NO] \leq 1 \times 10^{13}$ molecules/cm^3 and $5 \times 10^{11} \leq [NH_3] \leq 2 \times 10^{12}$ molecules/cm^3.

Reactants and products were detected mass spectrometrically, using modulated molecular beam sampling of the flow tube. The mass spectrometer was doubly-differentially pumped, with a 1- or 2-mm nozzle, 1-mm skimmer (Beam Dynamics), and 1.5-mm collimating orifice. An electron energy of 18 eV and an emission current of 0.75 mA were used in this study. $^{15}N^{14}N^{18}O$, $^{15}N^{14}N$, and $D_2{}^{18}O$ (or $H_2{}^{18}O$) ions were pulse counted, using an SRS 400 gated photon counter interfaced to an IBM AT computer. Modulated beam sampling with ac detection of the ion signals considerably improved the S/N, as well as offering a large measure of immunity from changes in background gas composition.

NH radicals were formed by the reaction of NH_3 with excess F atoms.[21,22] F atoms were formed by microwave discharge of a highly dilute F_2/He mixture using a Beenakker-type microwave cavity operating at 30–40 W of microwave power.

Reagents used were NH_3 (Matheson), ND_3 (MSD Isotopes), $^{15}N^{18}O$ (Isotec), N_2O (Matheson), N_2 (Scott Specialty Gases, 99.9995%), 5% F_2/He (Spectra Gases), and He (Matheson, 99.9999%). All reagents were used without further purification. Before experiments with ND_3 the flow system was deuterated by passing D_2O through it overnight.

Computational Details

Calculations were carried out using the Gaussian 90[23] and Gaussian 92[24] programs. We used the G2 method, as outlined by Pople and co-workers.[25] G2 uses a series of calculations to approximate a QCISD(T)/6-311+G(3df,2p)//MP2/6-31G(d) calculation with an additional "higher-order correction" based on the number of paired and unpaired electrons. In brief, G2 energies were obtained by following these steps: (1) Vibrational frequencies and zero-point energies were determined by scaling the results of HF/6-31G(d)//HF/6-31G(d) calculations. (2) Geometries were optimized at MP2/6-31G(d) level. (3) Energies were calculated using MP4/6-311G(d,p)//MP2/6-31G(d). (4) Corrections due to basis set incompleteness were evaluated by MP4/6-311+G(d,p)//MP2/6-31G(d), MP4/6-311G(2df,p)//MP2/6-31G(d), and MP2/6-311+G(3df,2p)//MP2/6-31G(d). (5) Corrections due to further electron correlation were evaluated by QCISD(T)/6-311G(d,p)//MP2/6-31G(d). (6) "High-level corrections" were evaluated based on the number of α and β valence electrons.

The method has been shown to yield atomization energies with a average absolute deviation of 0.9 kcal/mol for a large number of species containing first-row elements. We have carried out additional studies of the applicability of the G2 method to transition-state structures.[26] We found that it performed well in predicting transition-state properties, although its performance for transition states could be enhanced by using QCISD/6-311G(d,p) optimized geometries and frequencies instead of the MP2 optimized geometries and scaled Hf frequencies of the G2 method. We have used this G2//QCISD/6-31G(d,p), or G2Q, method to characterize the transition states leading to N_2 + OH and H + N_2O.

Results and Discussion

Experiment. We measure the branching fraction of the title reactions directly, using mass spectrometric detection of the stable reaction products, N_2O and N_2. NH (ND) is mixed with an excess of NO, driving the reaction rapidly to completion. The resulting gas mixture is sampled using molecular beam sampling and analyzed using mass spectroscopy. Relative detection efficiencies for the various species were measured directly using calibration mixtures containing known partial pressures of each of the stable species detected.

We use the reaction of ammonia with excess fluorine atoms as our NH radical source. This source was used by Hack et al.[22] in a study of the reaction of NH($^3\Sigma$) with $O_2(^1\Delta)$. They found that it was possible to make a sizable excess of NH over NH_2 by proper choice of the $[NH_3]/[F]$ ratio. There are, unfortunately, constrainst which limit the maximum $[NH_3]_0$ and hence the maximum [NH] possible. The first is the well-known production of solid NH_4F if the concentrations of NH_3 and HF become too high.[27] We also observed production of N_2H_x species for $[NH_3]_0 > 2.5 \times 10^{12}$ molecules/cm^3. To avoid these problems, we used low concentrations of ammonia, $5 \times 10^{11} \leq [NH_3]_0 \leq 2 \times 10^{12}$ molecules/cm^3. The $[NH_3]/[F]$ ratio was adjusted by adjusting [F] to achieve a maximum in the N_2O signal.

The use of isotopically-labeled $^{15}N^{18}O$ allowed us to separate signal due to the NH + NO reaction from most background signals. This did not help to separate out contributions due to small amounts of NH_2 reacting with NO producing N_2 + H_2O. Approximately 30% of the signal at $m/e = 29$ ($^{15}N^{14}N$) was due to this reaction. To correct for it, we measured the $m/e = 20$ (22)/$m/e = 29$ ($H_2{}^{18}O$ ($D_2{}^{18}O$)/$^{15}N^{14}N$) ratio with $[F] \ll [NH_3]$, ensuring that no NH was present. This ratio, coupled with our measurement of $m/e = 20$ (22), allowed us to correct for this side reaction. In work with NH_3 there was a further complication, since $m/e = 20$ contains contributions from $H_2{}^{18}O$ and HF. We corrected for this by measuring $m/e = 20$ with NO on and off, but the additional source of error shows up as a larger uncertainty in our branching fraction measurement for NH relative to that for ND. The resulting product branching fractions, measured at room temperature, for production of N_2O + H(D) were 0.84 ± 0.4 for NH($^3\Sigma^-$) + NO and 0.87 ± 0.17 for ND($^3\Sigma^-$) + NO (1σ statistical errors).

There have been reports that the excess-F + NH_3 system produces NH($^1\Delta$) in addition to NH($^3\Sigma$).[28] In order to rule out the NH($^1\Delta$) + NO reaction as a interference in this work, we substituted N_2 for He as carrier in a series of experiments. N_2 quenches NH($^1\Delta$), with a rate of $k_q = (6–9) \times 10^{-14}$ cm^3/(molecules s),[29] fast enough to ensure that all the NH($^1\Delta$) produced in the source is quenched to NH($^3\Sigma$) before addition of NO. The substitution did not affect the measured branching fraction, demonstrating that the product branching fraction measured here is unaffected by the possible presence of NH($^1\Delta$).

Theory. Addition of NH($^3\Sigma$) to NO($^2\Pi$) gives rise to 12 surfaces. In C_1 symmetry these are two doubly-degenerated ^{2}A surfaces and two 4-fold-degenerate ^{4}A surfaces. Since connecting the quartet surfaces with the ground-state products violates spin conservation, we will not consider the quartet surfaces further. Fueno et al.[17] have calculated structures for the *cis*- and *trans*-HNNO equilibrium geometries and find them to be planar, of ^{2}A′ and ^{2}A″ symmetries (C_s point group). Patel-Misra and Dagdigian's[15] analysis of the OH product from the NH($^3\Sigma$) + NO reaction leads them to also conclude that the transition state for the N_2 + OH product channel is planar. Fueno et al.[17] found the ^{2}A′ surface to be more stable than the ^{2}A″ surface, in agreement with Melius[16] and later work by Walch.[19] Walch[19] has examined the correlations between the HNNO surfaces and products. He concluded that the ^{2}A″ surface does not correlate with H + N_2O and is unfavorable toward formation of N_2 + OH, while the ^{2}A′ could lead to both product channels. We have

TABLE 1: G2 Energies[a]

species	E[MP4/6-311G9d,p)][b]	Δ(+)[c]	Δ(2df)[c]	Δ(QCI)[c]	Δ(G2)[c]	Δ(HLC)[c]	Δ(ZPE)	G2 energy[b]
N_2O	−184.311 97	−7.37	−99.18	19.53	9.13	−40.00	10.99	−184.437 13
trans-HNNO	−184.821 84	−11.17	−100.00	−5.01	−11.70	−40.19	18.61	−184.971 31
cis-HNNO	−184.815 88	−8.62	−99.51	−2.88	−11.56	−40.19	18.61	−184.960 03
trans-HN–NO	−184.702 99	−12.92	−97.61	−32.37	−10.82	−40.19	14.87	−184.882 03
cis-HN–NO	−184.706 86	−12.53	−95.36	−26.01	−10.79	−40.19	14.29	−184.877 46
cis–trans ts	−184.784 41	−9.05	−102.10	−0.94	−11.60	−40.19	17.06	−184.931 24
HN–OH(^{2}A′)	−184.753 05	−8.62	−99.19	−8.51	−9.87	−40.19	12.03	−184.907 40
QCISD/6-311G(d,p)	−184.748 63	−9.29	−98.25	−19.15	−9.71	−40.19	14.53	−184.910 69
H–NNO(^{2}A′)	−184.770 77	−8.16	−102.29	−1.85	−9.84	−40.19	10.77	−184.922 33
QCISD/6-311G(d,p)	−184.767 92	−7.89	−101.84	−6.84	−9.75	−40.19	11.97	−184.922 46

[a] The notation used is as follows: Δ(+) = E[MP4/6-311+G(d,p)] − E[MP4/6-311G(d,p)]; Δ(2df) = E[MP4/6-311G(2df,p)] − E[MP4/6-311G(d,p)]; Δ(QCI) = E[QCISD(T)/6-311G(d,p)] − E[MP4/6-311G(d,p)]; Δ(G2) = E[MP2/6-311+G(3df,2p)] − E[MP2/6-311G(2df,p)] − E[MP2/6-311+G(d,p)] + E[MP2/6-311G(d,p)]; Δ(HLC) = −0.19 × number of α valence electrons − 4.81 × number of β valence electrons; Δ(ZPE) = scaled zero-point vibrational energy; G2 energy = E[MP4/6-311G(d,p)] + Δ(+) + Δ(2df) + Δ(QCI) + Δ(G2) + Δ(HLC) + Δ(ZPE). [b] Energies in hartrees. [c] Energies in millihartrees.

TABLE 2: Calculated G2 Geometries and Frequencies (^{2}A′ Surface)[a]

	N_2O	*cis*-HN–NO	*trans*-HN–NO	*cis*-HNNO	*trans*-HNNO	*cis-trans* ts	NN–OH	H–NNO
r(NN)	1.171	1.902	1.911	1.186	1.196	1.186	1.157	1.129
r(NO)	1.192	1.165	1.162	1.210	1.194	1.199	1.454	1.197
r(NH)		1.041	1.036	1.038	1.023	1.049	1.203	1.423
∠HNN		92.8	96.2	111.2	109.4	112.8	94.2	116.8
∠NNO	180.0	119.5	125.0	143.1	137.9	177.0	96.4	168.6
ω_1	2633	683i	628i	3600	3713	3376	2421i	1286i
ω_2	1392	3212	3251	1640	1562	1976	1765	1830
ω_3	689	1552	1658	1449	1422	1437	1280	1173
ω_4		936	903	1167	1125	1143	805	759
ω_5		317	348	353	322	905i	471	375
ω_6		253	361	941	1005	455	958	590

[a] Distances are in angstroms, angles in degrees, and frequencies in cm^{-1}.

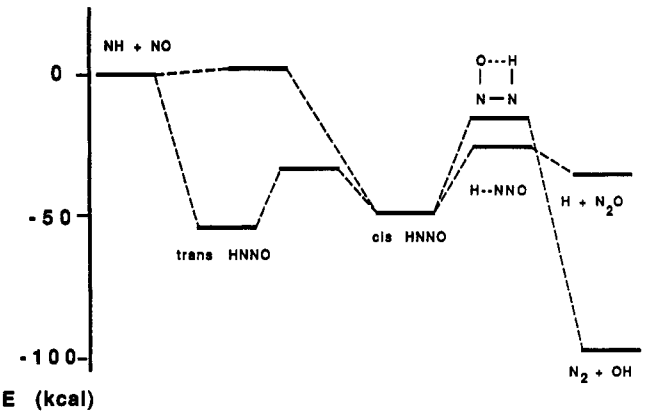

Figure 1. Schematic potential energy surface for HNNO(^{2}A′).

TABLE 3: Calculated G2Q Geometries and Frequencies (^{2}A′ Surface)[a]

	NN–OH	H–NNO
r(NN)	1.215	1.152
r(NO)	1.423	1.191
r(NH)	1.245	1.547
∠HNN	89.2	111.3
∠NNO	96.1	167.4
ω_1	2035i	1401i
ω_2	2113	2173
ω_3	1665	1288
ω_4	1015	764
ω_5	665	411
ω_6	919	619

[a] Distances are in angstroms, angles in degrees, and frequencies in cm^{-1}.

therefore focused on characterizing the ^{2}A′ surface. G2 calculations were utilized for most of the points on the surface; G2(Q) calculations were carried out for the transition states leading to N_2 + OH and N_2O + H. The surface is shown schematically in Figure 1.

Geometries, frequencies, and energies for the stationary points located on the HNNO ^{2}A′ potential energy surface can be found in Table 1–3. By combining these with other calculated G2 energies,[25] we can evaluate the energies for the stationary points on the HNNO ^{2}A′ surface. These values can be found in Table 4. We find very good agreement between our results and experimental energetics for the overall exothermicities of the reaction.

Table 4 also lists the energetics calculated previously by other workers. The quality of previous calculations, as judged from the calculated exothermicities of the reaction, varies widely. The studies by Fueno et al.[17] and Harrison and MacIagan[18] utilized small basis sets and low levels of theory and only qualitatively reproduce the overall reaction exothermicities. There is uniformity in predicting that the transition state for the H + N_2O channel is below that the N_2 + OH channel and general agreement that both channels are thermodynamically open. We agree with Walch[19] and disagree with BAC-MP4[4,16] in predicting that the *trans*-HNNO isomer is more stable than the *cis* isomer. Unfortunately, there is no experimental data on HNNO with which to compare. We find that Walch's [19] energies are uniformly 2.5 −4.5 kcal/mol higher than our G2(Q) results. Also, his energy for (N_2O + H) relative to (NH + NO) is 3.0 kcal/mol higher than experiment. We believe that the source of this error lies in his calculation of E(NH+NO) relative to the rest of the surface. An analogous situation exists in the case of the NH_2 + NO surface, where Walch has chosen to use the experimental heat of reaction to position of NH_2 + NO asymptote.[30] If we lower his reported energies by 3.0 kcal, the agreement between his work and the present work becomes quite good.

If we wish to describe the product branching fraction for the NH + NO reaction, we need to first consider the products of decomposition of the initially formed HNNO ^{2}A′ adducts. The presence of a barrier in the channel forming *cis*-HNNO suggests that substantial amounts of *trans*-HNNO will be formed. Geometry rules out a 1,3-hydrogen transfer, followed by formation of OH and N_2, for the *trans*-HNNO isomer. We also found that extension of the H–N bond leads to a lowering of the barrier to

TABLE 4: Energetics of HNNO Species[a]

cis-NNO	*trans*-HNNO	*cis*-HN–NO	*trans*-HN–NO	N_2–OH ts	H–N_2O ts	*cis–trans* ts	N_2 + OH	N_2O + H	reference
–48.9	–56.0	2.9	0.1	–17.9[e]	–25.3[e]	–30.8	–96.9	–34.5	this work
–46.2	–51.5	6.3	3.2	–15.4	–21.4			–31.7	19
–51.9	–48.8			–22.4	–28.2		–99.1	–37.6	4
–30.9				3.0	–6.9		–90.8	–28.9	18[b]
–29.5				3.6	–3.8		–91.6	–20.5	18[c]
–60.3	–60.5			–9.0	–12.2	–28.7	–92.4	–30.9	17
–50.2	–47.3			–17.3	–27.7		–97.5	–31.4	16
							–97.6	–34.7	experiment[d]

[a] All energies in kcal/mol, relative to NH + NO, 0 K. [b] MP4/6-31G(d)//MP2/6-31G(d). [c] MP4/6-311G(d,p)//HF/6-311G(d,p). [d] ΔH_f(NH) from ref 1; all other ΔH_f from JANAF tables.[2] [e] G2Q energy.

cis–trans isomerization, with the barrier disappearing before the N-H bond breaks. Therefore, we conclude that the only product arising from *trans*-HNNO is *cis*-HNNO. The barrier to *cis–trans* isomerization is low enough, relative to the barriers to dissociation, that we expect that the *cis* and *trans*-HNNO will be in equilibrium, and the product branching fraction will be described by the products of dissociation of cis-HNNO. On the basis of the relative locations of the transition states leading to N_2O + H and N_2 + OH, we would predict that the reaction of NH + NO would form predominantely H + N_2O products. Miller[31] has performed branching fraction calculations following the methodology used in his theoretical study of this reaction[4] and predicts, using G2 energies, a branching fraction of 0.89 for the N_2O + H channel, in good agreement with out experimental result. He has additionally calculated a deuterium kinetic isotope effect of 0.96, which agrees with the lack of an experimentally observed isotope effect.

Conclusion

We have directly measured the product branching fraction for the NH(D)($^3\Sigma$) + NO → products reaction at room temperature. We find that predominant, but not exclusive, production of N_2O + H (D). We do not see an observable deuterium kinetic isotope effect in the product branching fractions. We have additionally used G2 and G2Q to characterize a number of stationary points on the HNNO($^2A'$) surface. The exothermicities derived from this surface are in good agreement with experimental values. The shape of the G2(Q) surface is in good agreement with the recent CASSCF/CCI results of Walch,[19] especially if we lower his surface 3.3 kcal/mol, to bring the CASSCF/CCI exothermicity for the H + N_2O channel into agreement with the experimental value.

Acknowledgment. We thank Dr. J. A. Miller for helpful discussions and for performing the product branching fraction calculations using G2 input data. We also thank Dr. C. M. Rohlfing for helpful discussions. Finally, we thank E. B. Bochenski for his expert technical assistance and S. Dossa for his assistance. This research was sponsored by the U.S. Department of Energy, Office of Basic Energy Sciences, Division of Chemical Science.

References and Notes

(1) Anderson, W. R. *J. Phys. Chem.* **1989**, *93*, 530.
(2) Chase, M. W.; et al. *J. Phys. Chem. Ref. Data* **1985**, *14* (Suppl. No 1).
(3) Miller, J. A.; Bowman, C. T. *Prog. Energy Combust. Sci.* **1989**, *15*, 287.
(4) (a) Miller, J. A.; Melius, C. F. *Symp. (Int.) Combust. [Proc.]* **1993**, *24*, 719. (b) Melius, C. F. Private communication.
(5) Gordon, S.; Mulac, W.; Nangian, P. *J. Phys. Chem.* **1971**, *75*, 2087.
(6) Hansen, I.; Höinghaus, K.; Zetzsch, C.; Stuhl, F. *Chem. Phys. Lett* **1976**, *47*, 370.
(7) Cox, J. W.; Nelson, H. H.; McDonald, J. R. *Chem. Phys.* **1985**, *96*, 175.
(8) Harrison, J. A.; Whyte, A. R.; Phillips, L. F. *Chem. Phys. Lett.* **1986**, *129*, 346.
(9) Yamasaki, K.; Okada, S.; Koshi, M.; Matsui, H. *J. Chem. Phys.* **1991**, *95*, 5087.
(10) Mertens, J. D.; Chang, A. Y.; Hanson, K.; Bowman, C. T. *Int. J. Chem. Kinet.* **1991**, *23*, 173.
(11) Yokoyama, K.; Sakane, Y.; Fueno, T. *Bull. Chem. Soc. Jpn.* **1991**, *64*, 1738.
(12) Dean, A. M.; Chou, M.-S.; Stern, D. *Int. J. Chem. Kinet.* **1984**, *16*, 633.
(13) Vandooren, J.; Sarkisov, O. M.; Balakhnin, V. P.; van Tiggelen, P. J. *Chem. Phys. Lett.* **1991**, *184*, 294.
(14) Sausa, R. C.; Anderson, W. R.; Dayton, D. C.; Faust, C. M.; Howard, S. L. *Combust. Flame*, in press.
(15) Patel-Misra, D.; Dagdigian, P. J. *J. Phys. Chem.* **1992**, *96*, 3232.
(16) Melius, C. F.; Binkley, J. S. *Symp. (Int.) Combust., [Proc.]* **1984**, *20*, 575.
(17) Fueno, T.; Fukuda, M.; Yokoyama, K. *Chem. Phys.* **1988**, *124*, 265.
(18) Harrison, J. A.; MacIagan, R. G. A. R. *J. Chem. Soc., Faraday Trans.* **1990**, *86*, 3519.
(19) Walch, S. P. *J. Chem. Phys.* **1993**, *98*, 1170.
(20) Durant, J. L. *J. Phys. Chem.* **1991**, *95*, 10701.
(21) Walther, C. D.; Wagner, H. Gg. *Ber. Bunsen-Ges. Phys. Chem.* **1983**, *87*, 403.
(22) Hack, W.; Kurzke, H.; Wagner, H. Gg. *J. Chem. Soc., Faraday Trans. 2* **1985**, *81*, 949.
(23) Frisch, M. J.; et al. *Gaussian 90*, Revision I; Gaussian, Inc.: Pittsburgh, PA, 1990.
(24) Frisch, M. J.; et al. *Gaussian 92*, Revision B; Gaussian, Inc.: Pittsburgh, PA, 1992.
(25) (a) Pople, J. A.; Head-Gordon, M.; Fox, D. J.; Raghavachari, K.; Curtiss, L. A. *J. Chem. Phys.* **1989**, *90*, 5622. (b) Curtiss, L. A.; Jones, C.; Trucks, G. W.; Raghavachari, K.; Pople, J. A. *J. Chem. Phys.* **1990**, *93*, 2537. (c) Curtiss, L. A.; Raghavachari, K.; Trucks, G. W.; Pople, J. A. *J. Chem. Phys.* **1991**, *94*, 7221.
(26) Durant, J. L.; Rohlfing, C. M. *J. Chem. Phys.* **1993**, *98*, 8031.
(27) Silver, J. A.; Kolb, C. E. *J. Phys. Chem.* **1982**, *86*, 3240.
(28) Temps, F. Private communication, 1992.
(29) Nelson, H. H.; McDonald, J. R.; Alexander, M. H. *J. Phys. Chem.* **1990**, *94*, 3291. Hack, W.; Wilms, A. *J. Phys. Chem.* **1989**, *93*, 3540. Bower, R. D.; Jacoby, M. T.; Blauer, J. A. *J. Chem. Phys.* **1987**, *86*, 1954. Freitag, F.; Rohrer, F.; Stuhl, F. *J. Phys. Chem.* **1989**, *93*, 3170.
(30) Walch, S. P. *J. Chem. Phys.* **1993**, *99*, 5295.
(31) Miller, J. A. Private communication.